Analysis on Acoustic Impedance Models in Namorado Oilfield, Campos Basin, Brazil

Mario Martins Ramos, Rodrigo Bijani (Observatório Nacional-ON/MCTIC, Rio de Janeiro, Brazil)

Abstract

This work is concerned with the reliability of two different models to compute acoustic impedances in the Namorado field, Campos Basin, Brazil. Poor data coverage and acquisition problems enhanced numerous models in the literature. To estimate acoustic impedances in a reliable framework, we use a petrophysical expression that directly estimates acoustic impedances without the need of density logs. In addition, we also discuss empirical expressions to compute compressional velocities and consequently acoustic impedance using density, gama ray and resistivity logs. To validate both models, we calculate the observed acoustic impedance directly from the elastic theory and also present 2-D maps of impedances for the whole Namorado field. The results show that both models are good for low values of impedance, despite of the overall sub-estimation of the acoustic impedance by the petrophysical model. The empirical model presents more dispersive estimations of acoustic impedance when faced with the observed impedance.

Introduction

The acoustic impedance is a rock property that directly involves density and velocity, both of which can be directly measured by well logging (Latimer et al., 2000; Yilmaz, 1991). The benefits of the acoustic impedance are notorious for many geophysical purposes. It is a key parameter for i) detecting variations of lithologies in depth, ii) investigating hydrocarbon fields and iii) exploiting offshore continental margins (Becquey et al., 1979; Mabrouk, 2010). The main concern about this work is presenting a comparative study on acoustic impedances applied for the Namorado Oilfield, in Campos Basin, Brazil. We begin by the usual definition of the acoustic impedance as a function of density and sonic logs. We then investigate the applicability of two different models to calculate acoustic impedances in the absence of density and sonic logs. The first model was proposed by Kamel and Mabrouk (2004) and is well-suited for computing the acoustic impedance in the absence of density log. The second investigated model is a proposition of Augusto (2009), which is based on a set of empirical expressions and the multi-linear regression to compute the compressional velocity V_p. To verify the ability of both models in predicting the realistic acoustic impedances, we compare the estimated and observed impedances for seven well logs with complete density and sonic data of Namorado Oilfield (see Figure 1). In section , we do the same comparisons for the lithology in order to investigate some specific bedding deposits in Namorado field. This work comes to an end with a brief discussion about general aspects of both models.

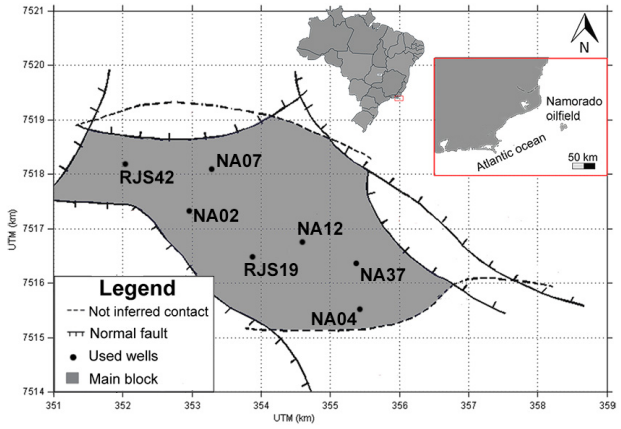

Figure 1 *– Location of the main block of Namorado Oilfield and the seven well logs explored in this work (Modified from Augusto 2009).*

Method

Let us assume an acoustic well log where bulk density (ρ_b) and sonic transit time (Δ_t) are measured in a well log. From elastic theory (Yilmaz, 1991), the acoustic impedance of a medium (Z) is given by:

$$Z = \frac{\rho_b}{\Delta_t}, \tag{1}$$

where ρ_b is the bulk density in g/cm^3 and Δ_t is the sonic transit time (Δ_t) in $\mu s/ft$. The sonic transit time is inversely proportional to the compressional velocity (V_p), as stated by the following expression:

$$\Delta_t = \frac{1}{V_p}. \tag{2}$$

In this work, we refer to observed acoustic impedance (Z_{obs}) as the one computed directly by ρ_b and Δ_t logs. Due to problems during the acquisition process and other logistical issues, it is common to have lack of measurements or even omitted logs in different acoustic well logs. To overcome this obstacle, different models were proposed in the literature (hua Han et al. (1986), Gardner et al. (1974)). In here, we have investigated two approaches. The first one is a set of empirical expressions, proposed by Augusto (2009) to compute compressional velocities (V_p) in the absence of the Δ_t profile. The second

approach was proposed by Kamel and Mabrouk (2004) to calculate acoustic impedances from well logs with a lack of measured ρ_b.

Firstly, we apply the referred models to seven acoustic well logs of Namorado field in order to analyse similarities and discrepancies of modelled impedances and the observed impedance Z_{obs}. A brief discussion about the methods of Augusto (2009) and Kamel and Mabrouk (2004) are presented In following Sections.

Empirical Model

Suppose that there is an acoustic well log with missing Δ_t log. In this case, the computation of the acoustic impedance by Equation 1 depends on the estimation of Δ_t (or V_p) by means of a model. In this work, the empirical model of Augusto (2009) is applied for the well logs highlighted in Figure 1. The method consists in computing the compressional velocity (V_p) by seven empirical expressions for each well involving other available petrophysical logs, like gama-ray, density, resistivity and porosity. Once (V_p) is computed for each acoustic well log, we then use Equation 1 to obtain the empirical acoustic impedance (Z_e). From hereinafter, the subscript $_e$ states for the empirical model of (Augusto, 2009).

Kamel and Mabrouk Model

In the absence of bulk density logs, Kamel and Mabrouk (2004) developed an analytical expression to calculate the acoustic impedance as a function of Δ_t and other petrophysical quantities. The basis of Kamel and Mabrouk (KM) model are related to the analysis of effective porosities from sonic and density logs, as presented by the following extended expression:

$$Z_{KM} = \frac{1}{\Delta_t}\left[\left\{V_{sh}\left(\frac{\rho_{sh}-\rho_{ma}}{\rho_f-\rho_{ma}} - \frac{\Delta_{tsh}-\Delta_{tma}}{\Delta_{tf}-\Delta_{tma}}\right) + \frac{\Delta_t-\Delta_{tma}}{\Delta_{tf}-\Delta_{tma}}\right\}(\rho_f-\rho_{ma}) + \rho_{ma}\right], \quad (3)$$

where Δ_t is the slowness measured along the well, $\Delta_{tma} = 169\ \mu s/m$ and $\rho_{ma} = 2.65\ g/cm^3$ are the slowness and the density of the rock matrix, $\Delta_{tsh} = 396\ \mu s/m$ and $\rho_{sh} = 2.4\ g/cm^3$ are the slowness and the density of the shale, $\Delta_{tf} = 564\ \mu s/m$ and $\rho_f = 1.1\ g/cm^3$ are the slowness and the density of the fluid. The shale volume (V_{sh}) is computed from available gamma ray log using Schlumberger (1975) and corrected by Larionov (1969). All the values listed above are extracted from Kamel and Mabrouk (2004). As stated in the end of this Section, to apply the KM model for the Namorado Oilfield, we use Equation 3 for the same acoustic logs presented in Figure 1. From hereinafter, the subscript $_{KM}$ is related to the Kamel and Mabrouk model.

Maps

Once we have computed Z_{obs}, Z_e and Z_{KM} for each of the seven acoustic well logs of Namorado Oilfield, we present 2-D impedance maps of Z_{obs}, Z_e and Z_{KM} at specific depths to discuss the lateral variations of such parameter and again verify the similarities among modelled and observed impedance. For this purpose, we implement the simple kriging interpolation algorithm based on Krige (1951), Sarma (2010), Isaaks and Srivastava (1989).

Results

To verify the applicability of the presented methodology, we compare modelled Z_{KM} and Z_e values with the observed acoustic impedance Z_{obs} for two wells of Namorado Oilfield (NA02, NA04).

NA02

We start with well log NA02. Figure 2 (a) and (b) present the comparison of Z_{obs}, Z_{KM} and Z_e in scatter plots. It is possible to observe a better accordance between the observed impedance Z_{obs} and the Impedance computed by KM model (i.e., when density profile is absent). The r value presented in Figure 2 (a) shows a better correlation between Z_{obs} and Z_{KM}, indicating a fewer dispersion between Z_{obs} and Z_{KM}. This figure also shows a better correlation when the main lithology are sandstones. Figure 2 (b) shows that the empirical model could not estimate high Z values (i.e., above 4.0 x 10^4 $ft/s.g/cm^3$) and shows also a high dispersion for non-sandstone rocks. This feature indicates that, for well log NA02, the KM model represents the observed impedance more accurately than the impedance computed by empirical model (Z_e).

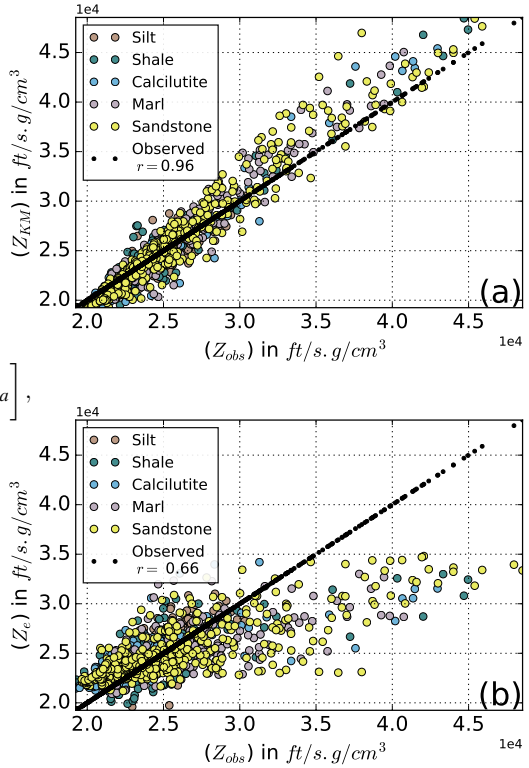

Figure 2 *– (a) Scatter plot of Z_{obs} (black dots) versus Z_{KM} (colored dots) and (b) Z_{obs} versus Z_e (colored dots) for well log NA02 of Namorado Oilfield. The colors of both models are respective for the lithology. The r values in legends represent the correlation coefficient between Z_{obs} and the respective model. Optimal correlation is when $r = 1.0$.*

To analyse the behaviour of the acoustic impedance in depth, we also present the impedance profile of well log NA02, ranging from 2950 to 3150 meters depth. Figure 3 (a) present the comparison of Z_{obs}, Z_{KM} and Z_e. In general,

there is a reasonable fit between Z_{obs} and Z_{KM}, which reinforces the validation of KM model for well log NA02.

There are several interbedded deposits along this profile involving sandstone, calcilutite, shale and marl, as exhibited in legend of Figure 3 (b).

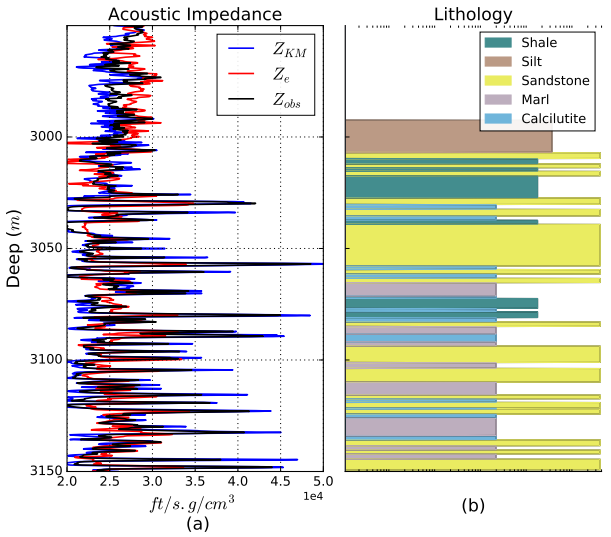

Figure 3 *– (a) Variations of acoustic impedances values in depth, (b) the lithological information collected from well NA02.*

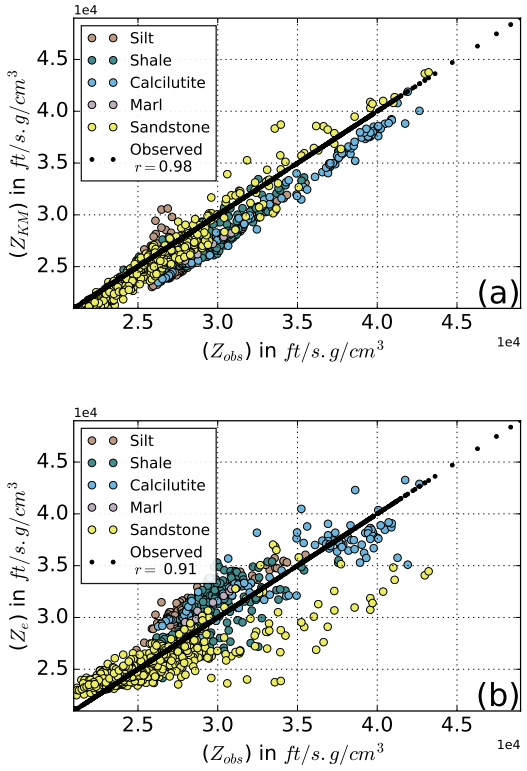

Figure 4 *– (a) Scatter plot of Z_{obs} (black dots) versus Z_{KM} and (b) Z_{obs} versus Z_e for well log NA04 of Namorado Oilfield. The colors of both models are respective for the lithology. The r values in legends represent the correlation coefficient between Z_{obs} and the respective model. Optimal correlation is when $r = 1.0$.*

NA04

Now we present the same sequence of images for the well log NA04. The location of such well log in Namorado field can be seen in Figure 1. In this case, we can see in Figure 4 (a) and (b) that the scatter plots of Z_{KM} and Z_e present similar features, corroborated by the high correlation coefficient values (i.e., $r = 0.91$ for Z_e and $r = 0.98$ for Z_{KM}) and a better correlation in sandstones.

Figure 5 (a) present the variation in depth of acoustic impedances of both Z_{KM} and Z_e when compared to Z_{obs}. It is interesting to observe that the high Z_{obs} values (i.e., around 4.5 x 10^4 $ft/s\ g/cm^3$) are not well estimated by Z_e. There are two abrupt changes in Z values around depths 3025 and 3112, as shown in Figure 5 (a).

Additionally, Figure 5 brings complementary information about the lithological group of well log NA04. As can be seen in Figure 5 (b), Z_{obs}, Z_{KM} and Z_e curves present reasonable similarities along the profile NA04 mainly for sandstones.

2D Impedance Maps

In this section we present an overall view of 2-D impedance maps of Namorado Oilfield produced by observed and modelled values at three specific depths (i.e., a shallow depth at 2974 m, an intermediate depth at 3038 m and a deep depth at 3103 m, respectively). It is mentionable that we have few data (only seven logs) for presenting a robust 2-D impedance map. Despite, we believe that some in sites about the 2-D distribution of impedances for the other logs of Namorado Oilfield are required.

2974 m Depth

The first set of 2-D impedance maps for depth 2974 m are presented in Figure 6 (a), (b) and (c). There are reasonable similarities between Z_{obs}, Z_e and Z_{KM} nearby well logs NA07, NA37. Some wells are drawn in white for visibility.

3038 m Depth

In Figure 7 (a), (b) and (c), we present the 2-D acoustic maps for the 3038 m depth. There are good accordances among Z_{obs}, Z_{KM} and Z_e values specifically in regions surrounding well logs NA02, NA37 and NA04. There are overestimation of Z_e in well log RJS19 and underestimation of Z_{KM} in well log RJS42.

3103 m Depth

The last 2-D acoustic maps are presented in Figure 8 (a), (b) and (c). In this case, we observe good similarities in Z_e and Z_{obs} maps, specially for well logs RJS42, NA02 and RJS19. The Z_{KM} values at this depth are in general underestimated. This could be related to some unrealistic estimated impedance values in regions where pores have low-density gas (Kamel and Mabrouk, 2004).

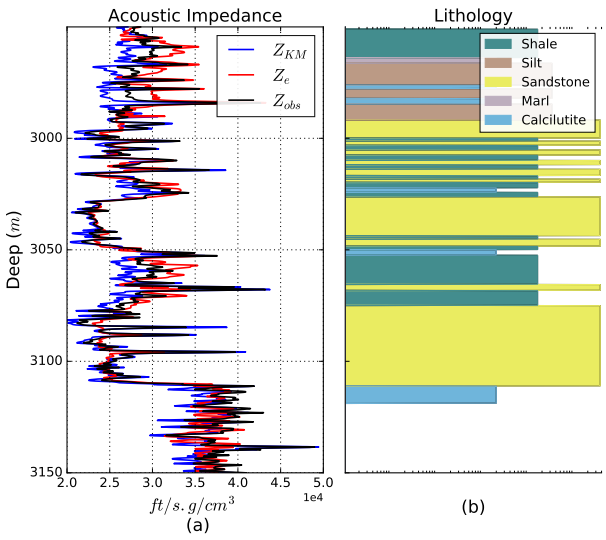

Figure 5 *– (a) Variations of acoustic impedances values in depth, (b) the lithological information collected from well NA04.*

Conclusions

In this work we have compared the observed acoustic impedance (computed from full density and sonic logs) with that computed from two different models. The first model is a mathematical expression proposed in the KM model involving sonic and gamma ray logs that presented reasonable agreement with the observed data for the discussed well logs of Namorado Oilfield (i.e., NA02 and NA04). The KM model shows good response for Namorado Oilfield and seems to be a very good option for those logs with missing density data. The second is a set of empirical expressions to predict sonic logs by using the other available log measurements (i.e., effective porosity, gamma ray and electrical resistivity). The application of the empirical model to Namorado Oilfield showed some discrepancies between observed and modelled acoustic impedances, specially at high values of Z that are related manly to sandstones. This better results for a specific lithology shows also that both models were made for reservoir rocks, mainly sandstones.

We believe that a possible extension of this work would be the application of KM model to the set of missing (or incomplete) density profiles of Namorado Oilfield (13 in our case). We also believe that another method for modelling sonic logs might increase the quality of estimated impedances and consequently lead to more accurate 2-D or even 3-D impedance maps of the whole Namorado Oilfield.

Acknowledgments

We appreciate CAPES and CNPQ for the assistance provided in the development of this work.

References

Augusto, F. O. A. (2009). Mapas de amplitude sísmica para incidência normal no reservatório namorado, bacia de campos. Ph.D. dissertation, Observatório Nacional (ON), Rio de Janeiro, Rio de Janeiro, Brasil.

Becquey, M., Lavergne, M., and Willm, C. (1979). Acoustic impedance logs computed from seismic traces. *Geophysics*, 44(9):153–172.

Gardner, G. H. F., Gardner, L. W., and Gregory, A. R. (1974). Formation velocity and density - the diagnostic basics for stratigraphic traps. *Geophysics*, 39(6):770–780.

hua Han, D., Nur, A., and Morgan, D. (1986). Effects of porosity and clay content on wave velocities in sandstones. *Geophysics*, 51:2093–2107.

Isaaks, E. H. and Srivastava, R. (1989). *Applied Geostatistics*. Oxford University Press, 1 edition.

Kamel, M. H. and Mabrouk, W. M. (2004). Estimating seismic impedance and elastic parameters in hydrocarbon-bearing reservoirs from acoustic logs. *Journal of Petroleum Science and Engineering*, 45:21–29.

Krige, D. G. (1951). A statistical approach to some basic mine valuation problems on the witwatersrand. *Journal of the Chemical, Metallurgical and Mining Society of South Africa*, 52:119–139.

Larionov, V. (1969). Borehole radiometry. *U.S.S.R., New England Development Research Association - Nedra*.

Latimer, R., Davidson, R., and van Riel, P. (2000). An interpreter's guide to understanding and working with seismic-derived acoustic impedance data. *Geophysics*, 19(3):242–256.

Mabrouk, W. M. (2010). Acoustic impedance inversion approach from petrophysical data. *Journal of Petroleum Science and Engineering*, 73:181–184.

Sarma, D. (2010). *Geostatistics with Applications in Earth Sciences*. Springer.

Schlumberger (1975). A guide to wellsite interpretation of the gulf coast. *Schlumberger Well Services*.

Yilmaz, Ö. (1991). *Seismic Data Processing*. Investigations in geophysics. Soc. of Exploration Geophysicists.

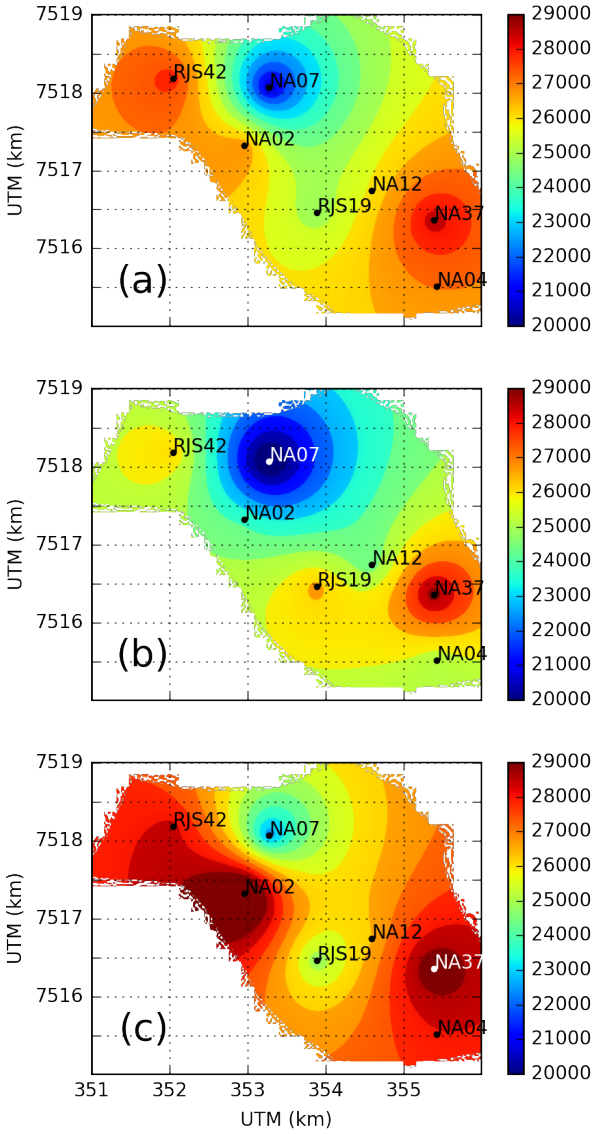

Figure 6 *– 2-D Acoustic Impedance $(ft/s\ g/cm^3)$ maps produced from (a) Z_{obs}, (b) Z_{KM} and (c) Z_e at $2974\ m$ depth. Each well log is identified to show the location in Namorado field.*

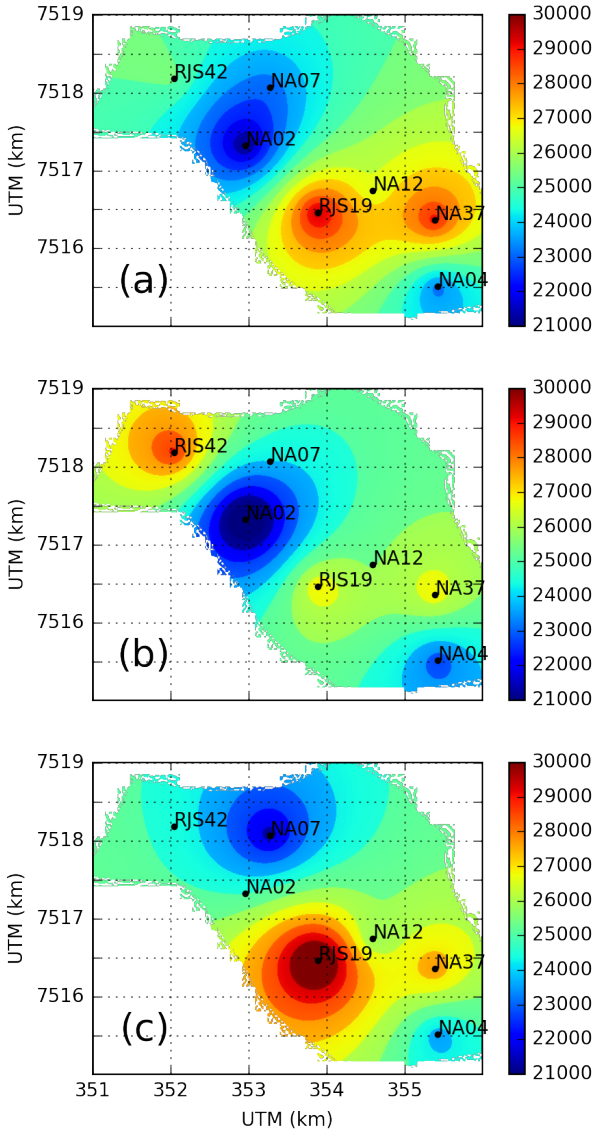

Figure 7 *– 2-D Acoustic Impedance $(ft/s\ g/cm^3)$ maps produced from (a) Z_{obs}, (b) Z_{KM} and (c) Z_e at $3038\ m$ depth. Each well log is identified to show the location in Namorado field.*

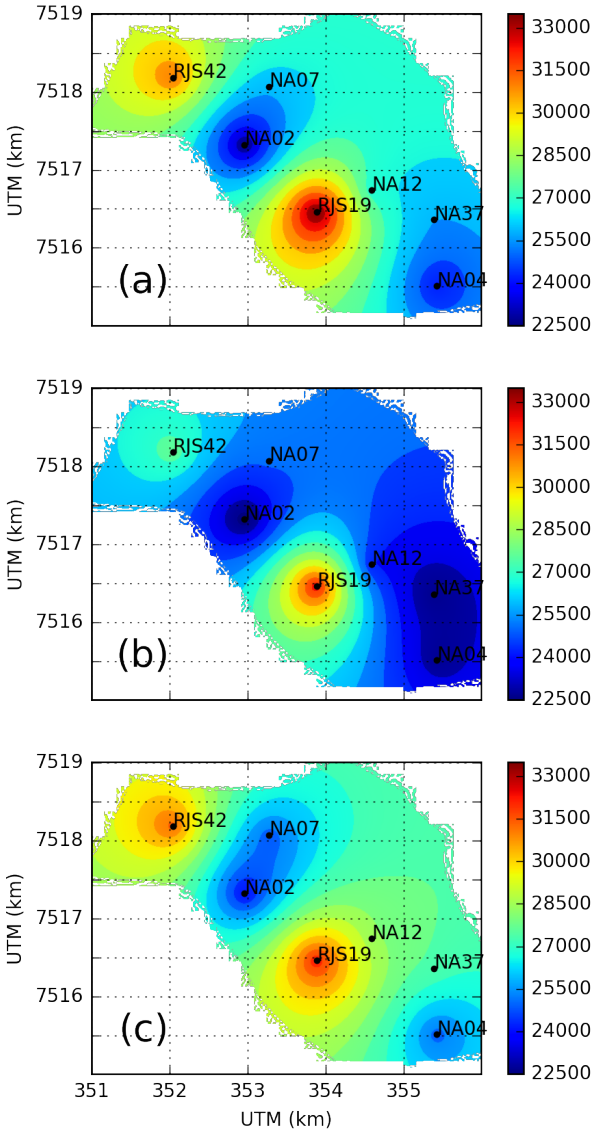

Figure 8 *– 2-D Acoustic Impedance* $(ft/s\ g/cm^3)$ *maps produced from (a)* Z_{obs}*, (b)* Z_{KM} *and (c)* Z_e *at* $3103\ m$ *depth. Each well log is identified to show the location in Namorado field.*